Neuron
Report

Blocking Endocytosis Enhances Short-Term Synaptic Depression under Conditions of Normal Availability of Vesicles

Yunfeng Hua,[1,2] Andrew Woehler,[1,4] Martin Kahms,[2] Volker Haucke,[3] Erwin Neher,[1,4,*] and Jürgen Klingauf[2,5,*]
[1]Department of Membrane Biophysics, Max Planck Institute for Biophysical Chemistry, 37077 Göttingen, Germany
[2]Department of Cellular Biophysics, Institute for Medical Physics and Biophysics, University of Münster, 48149 Münster, Germany
[3]Department of Molecular Pharmacology & Cell Biology, Leibniz Institut für Molekulare Pharmakologie, 13125 Berlin, Germany
[4]Center Nanoscale Microscopy and Molecular Physiology of the Brain (CNMPB), 37073 Göttingen, Germany
[5]Cluster of Excellence EXC 1003, Cells in Motion, CiM, 48149 Münster, Germany
*Correspondence: eneher@gwdg.de (E.N.), klingauf@uni-muenster.de (J.K.)
http://dx.doi.org/10.1016/j.neuron.2013.08.010

SUMMARY

It is commonly thought that clathrin-mediated endocytosis is the rate-limiting step of synaptic transmission in small CNS boutons with limited capacity for synaptic vesicles, causing short-term depression during high rates of synaptic transmission. Here, we show by analyzing synaptopHluorin fluorescence that 200 action potentials evoke the same cumulative amount of vesicle fusion, irrespective of the frequency of stimulation (5–40 Hz), implying the absence of vesicle reuse, since the method used (alkaline-trapping) measures only first-round exocytosis. After blocking all slow or specifically clathrin-mediated endocytosis, however, the same stimulation patterns cause a rapid stimulation-frequency-dependent release depression. This form of depression does not reflect insufficient vesicle supply, but appears to be the result of slow clearance of vesicular components from the release site. Our findings uncover an important yet overlooked role of endocytic proteins for release site clearance in addition to their well-characterized role in endocytosis itself.

INTRODUCTION

In many types of synapses the level of neurotransmitter release during ongoing activity may be limited by the availability of release-ready vesicles and, therefore, depends on the speed of vesicle recruitment. Surprisingly, many synapses in the central nervous system can sustain synaptic activity upon high-frequency stimulation (Kopp-Scheinpflug et al., 2008; Kraushaar and Jonas, 2000; Lorteije et al., 2009; Rancz et al., 2007). In order to maintain the fidelity of synaptic transmission, synaptic vesicles (SVs) are required to undergo fast recycling to prevent depletion of the SV pool (Fernández-Alfonso and Ryan, 2004; Sudhof, 2004). Recently it has been reported that interfering with the function of endocytic proteins causes a fast, stimulation-frequency-dependent depression of SV exocytosis (Hosoi et al., 2009; Kawasaki et al., 2000). As obvious explanation for such findings, the lack of release-ready SVs may be invoked due to absence of recycled SVs. However, some of these inhibitory effects developed so rapidly that they cannot be explained by the lack of release-ready SVs, since the reservoir of SVs should well be able to maintain release for longer periods.

In this study we investigated vesicle exocytosis in cultured rat hippocampal neurons using synaptopHluorin (Miesenböck et al., 1998; Sankaranarayanan et al., 2000) in the presence of Folimycin, a potent and specific inhibitor of vesicular reacidification, that does not affect exo-endocytosis (Zhou et al., 2000). We demonstrate that upon mild stimulation no reuse of SVs occurs within 40 s and that recruitment of pre-existing SVs is fast enough to meet the needs of a high release rate. However, under the influence of the specific endocytosis inhibitor Dynasore (Macia et al., 2006) or the inhibitor of clathrin-mediated endocytosis Pitstop 2 (von Kleist et al., 2011) we observed a clear stimulation-frequency-dependent release depression. This probably reflects interference of these inhibitors with the process of rapid clearance of exocytosed SV components from the synaptic release sites. This notion was corroborated by the observation of acute vesicular protein accumulation around the release site using dual-color STED nanoscopy.

RESULTS

Limited Vesicle Reuse during Mild Stimulation

To reliably measure the level of synaptic release depression, we quantified the amount of exocytosis upon different stimulation strengths using synaptopHluorin (spH) in cultured hippocampal neurons (Miesenböck et al., 1998; Sankaranarayanan et al., 2000). At presynaptic terminals expressing spH, exocytosis of SVs evoked by electric field stimulation (via action potentials, APs) led to dequenching of spH molecules in neutral extracellular buffer, resulting in an instantaneous fluorescence increase (Figure 1A). Under such experimental conditions, the fluorescence change is proportional to the amount of spH exocytosed. The absolute amplitude of the signal can differ, however, from cell to cell due to inhomogeneous expression of the probe and variation in release probability. Therefore, we developed a

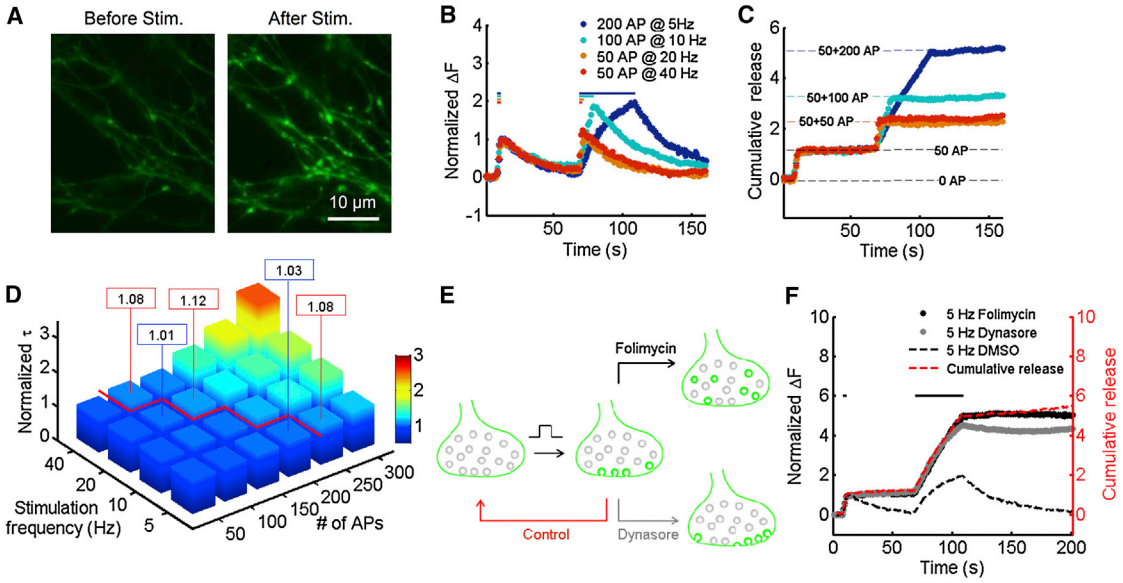

Figure 1. Normalized Cumulative spH Signal Increases Linearly with the Number of Stimuli

(A) Pseudo-color images of a spH-transfected hippocampal neuron, during rest (left) and after field stimulation with 200 APs at 20 Hz (right). Scale bar, 10 µm. (B) Representative spH responses to 50 APs at 20 Hz followed by 200 APs at 5 Hz (blue), 100 APs at 10 Hz (cyan), 50 APs at 20 Hz (orange), or 40 Hz (red). Between stimuli an interval of 60 s was given for recovery. Fluorescence transients are normalized to the response of the calibration stimulus. (C) Time courses of cumulative release calculated from (B). Decay phases of normalized fluorescence transients in (B) (calibration response) were fit with an exponential function (τ = 28.6 ± 0.8 s). Relative release rates of subsequent responses were calculated by deconvolution. Integrating the release rate time course provided a good estimation of cumulative release for quantitative comparison. (D) Endocytic time constants from synapses challenged with different stimulation protocols. Fluorescence decays were fit by a single exponential. Time constants are normalized to those of the calibration response. High stimulation rates and prolonged stimulation led to increased endocytic time constants (right side of the red borderline). Data points on the left side of the borderline have a difference less than 5%. (E) Schematic experimental design. Green color symbolizes fluorescent spH: during stimulation (arrow) newly exocytosed SVs become fluorescent; when endocytosed their fluorescence is quenched by reacidification (control) or stays (Folimycin). Under Dynasore they remain fluorescent at the plasma membrane. (F) Comparison of estimated cumulative release (200 APs, 5 Hz) using three different methods. Experiment in (C) was repeated in presence of 100 µM Dynasore (gray) or 80 nM Folimycin (black). Comparison of the deconvolved-integrated control signal (red, broken line, norm. release = 4.98 ± 0.30) with that from Folimycin (norm. release = 4.91 ± 0.19) and Dynasore (norm. release = 4.55 ± 0.33) experiments revealed only a small reduction for Dynasore treatment. See also Figures S1 and S2.

normalization procedure (see Supplemental Experimental Procedures for details). A calibration stimulus of 50 APs at 20 Hz is followed by a 60 s recovery interval and the test stimulus of interest. Fluorescence transients were normalized to the calibration response amplitudes, providing a signal that is independent of initial release probability and spH expression level (Figure 1B).

Since ongoing endocytosis during stimulation counteracts protein accumulation at the plasma membrane, spH fluorescence decreases in between stimuli, causing reduction of peak values in response to a given number of stimuli at low frequencies (Figure S1A, available online). In order to compensate for endocytosis and to further characterize the role of stimulation frequency on release rates, we developed a deconvolution routine, in which the normalized calibration response was taken as a replica for the elementary event (ee Supplemental Experimental Procedures for details). To validate this method we performed deconvolution on normalized fluorescence transients in Figure 1B. This analysis revealed stepwise increases in cumulative release rate during periods of stimulation and cumulative release was found to increase linearly with the number of APs for mild stimulation up to 200 APs at 5 Hz (Figure 1C), in agreement with previous studies using alkaline trapping (Ariel and Ryan, 2010; Li et al., 2005). However, we also observed that for stronger and longer-lasting stimulation, time constants of fluorescence decay upon exocytosis become larger, confirming earlier results regarding the limited capacity of endocytosis (Balaji and Ryan, 2007). This compromises the use of deconvolution, in which a time-invariant template is assumed. We, therefore, explored the range of constant decay rates (Figure 1D) and found that for a given number of APs the time constant is invariant up to a certain firing frequency, which was 5 Hz for 200 APs and 40 Hz for 50 APs (see Supplemental Experimental Procedures for details).

Despite its narrow range of applicability, the deconvolution method has an advantage over other methods, which either block compensatory endocytosis or prevent vesicular reacidification (alkaline-trapping), since it directly measures the rate of exocytosis without any perturbations. When applicable, it provides a better estimate for exocytosis, since it takes into account the contributions of reused SVs (Figure S2). In fact, comparing the results of deconvolution with those of using, e.g., alkaline-trapping should allow one to estimate the contribution of SV reuse. To do so, we next performed measurements with Folimycin (V-ATPase inhibitor) and Dynasore (dynamin GTPase inhibitor). The effects of these two inhibitors are schematically illustrated in Figure 1E. We found for 200 APs at 5 Hz the

fluorescence response in the presence of 80 nM Folimycin to be strikingly similar to the deconvolved-integrated signal obtained in the absence of the proton pump inhibitor. The amplitude with 100 μM Dynasore treatment was only slightly smaller (Figure 1F). In agreement with several previous studies (Betz and Bewick, 1993; Li et al., 2005; Wu and Wu, 2009), these findings demonstrate no major contribution of SV reuse to synaptic transmission within a 40 s period.

Block of Endocytosis Causes Release Depression

When stimulating at 10–100 Hz, a reduction in synaptic response (called short-term synaptic depression, STD) is observed in many types of glutamatergic synapses. Upon sustained stimulation, the rate of synaptic release drops rapidly and reaches a steady state within 10–20 stimuli, reflecting a balance between SV usage and recruitment of new SVs. To further examine the dynamics of SV cycling during stimulation with higher frequencies, we first repeated experiments by stimulating synapses with a fixed number of 200 APs with increasing frequency and in the presence of Folimycin (Figure 2A). Total fluorescence increases were found to be similar except for a slight decrease at 40 Hz. The similarity of cumulative amplitudes for 5, 10, and 20 Hz suggests that the same number of vesicles were trapped in the alkaline state, indicating the absence of significant STD and vesicle reuse.

Based on this finding we then tested whether STD is apparent after acute block of dynamin activity in primary neurons, as has been reported in the Calyx of Held (Hosoi et al., 2009). Indeed, in the presence of Dynasore the amplitude of fluorescence responses dropped monotonically with increasing stimulation frequency (Figure 2B). To confirm that this was Dynasore specific, we examined spH responses to 200 APs at 20 Hz in the presence of both Dynasore and Folimycin (Figure S3) or Folimycin alone. We found that addition of Folimycin did not cause similar STD. Neither did it rescue or enhance the STD caused by Dynasore. Furthermore, in order to explore the relationship between exocytic load and this type of STD, we reduced release probability by lowering external Ca^{2+} concentration from 2 mM to 1 mM. In the presence of Folimycin, the normalized amplitudes were as large as for 2 mM Ca^{2+} (Figure S4A), suggesting the same relative reduction in release rate during calibration and test stimulation. In the presence of Dynasore, however, similar amplitudes were found for 5 Hz stimulation (Figure S4B), while for 40 Hz the spH response was somewhat reduced, but much less than at 2 mM (Figure S4C), implying that the effect of Dynasore becomes weaker, when fewer vesicle components accumulate at the plasma membrane.

Since overexpression of pHluorin fusion constructs can result in an excess surface expression (Wienisch and Klingauf, 2006), which in turn might interfere with release site clearance and even induce the observed fast STD, we used two independent approaches not involving overexpression. First, we stained recycled vesicles with cypHer-labeled antibodies against the luminal domain of synaptotagmin 1 (αSyt1-cypHer) (Hua et al., 2011) and examined frequency-dependent STD (Figures 2C and 2D). Note that αSyt1-cypHer transients are mirror images of spH transients owing to the inverse pH dependence. In the presence of Dynasore, again we observed enhanced STD upon 40 Hz stimulation (Figure 2D). Second, to test whether the observed STD is specifically dependent on dynamin or more generally on the block of compensatory endocytosis, we used the recently described inhibitor of clathrin-mediated endocytosis, Pitstop, in its cell-membrane-permeable variant Pitstop 2 (von Kleist et al., 2011). Initial experiments using pH-switchable

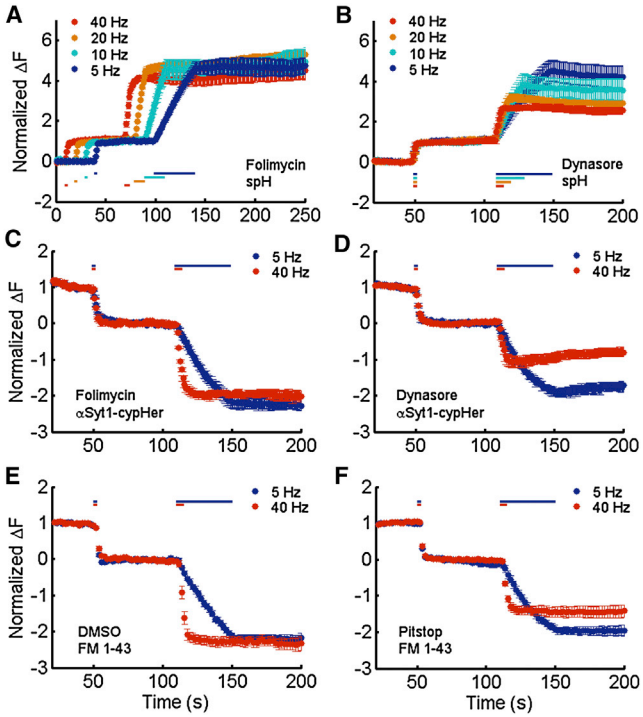

Figure 2. Frequency-Dependent Release Depression in the Presence of Dynasore, but Not Folimycin

(A) Average spH responses to 50 APs at 20 Hz followed by 200 APs at 5 Hz (blue), 10 Hz (cyan), 20 Hz (orange), or 40 Hz (red) in the presence of Folimycin (n = 6 each). Fluorescence transients were normalized to the calibration stimulus. The signal amplitude was insensitive to stimulus frequency (mean value of total fluorescence changes: 4.91 ± 0.19 for 5 Hz, 4.89 ± 0.33 for 10 Hz, 4.95 ± 0.17 for 20 Hz, and 4.39 ± 0.19 for 40 Hz). Traces are time shifted for better visibility. (B) As in (A, but in the presence of Dynasore (n = 5 trials each). Increased stimulation frequency led to a reduction in the signal amplitude (mean value of total fluorescence changes: 4.55 ± 0.33 for 5 Hz, 3.84 ± 0.34 for 10 Hz, 3.21 ± 0.10 for 20 Hz, and 2.66 ± 0.13 for 40 Hz). (C) Average cypHer responses to 50 APs at 20 Hz followed by 200 APs at 5 Hz (blue) or 40 Hz (red) in the presence of Folimycin (n = 6 each). Transients are normalized to the calibration stimulus. Similar signal amplitudes were observed (mean value of total fluorescence changes: 2.96 ± 0.095 for 40 Hz and 3.20 ± 0.15 for 5 Hz). (D) Same as in (C), but in the presence of Dynasore (n = 6 each). Stimulation at 40 Hz (red, mean value of total fluorescence changes: 2.05 ± 0.14) led to a reduction compared to 5 Hz (blue, mean value of total fluorescence changes: 2.86 ± 0.12). (E) Average FM1-43 destaining profiles in response to 50 APs at 20 Hz followed by 200 APs at 5 Hz (blue, n = 6, mean value of total fluorescence changes: 3.07 ± 0.09) or 40 Hz (red, n = 6, mean value of total fluorescence changes: 3.27 ± 0.12). Synaptic boutons were preloaded with FM dye by stimulation with 600 APs at 10 Hz. Transients are normalized to calibration stimulus. (F) Same as in (E), but in the presence of 30 μM pitstop (n = 6 each). Stimulation at 40 Hz (red, mean value of total fluorescence changes: 2.47 ± 0.13) led to a reduction compared to 5 Hz (blue, mean value of total fluorescence changes: 3.14 ± 0.10). All error bars represent SEM. See also Figures S3 and S4.

exo- and endocytosis markers like pHluorins and cypHer uncovered an unspecific side effect of Pitstop 2 on vesicular acidification as well as mitochondrial pH (M.K., M. Martineau, and J.K., unpublished data), thus precluding their use in conjunction with Pitstop 2. Therefore we stained SVs with the styryl dye FM1-43 and unloaded boutons with the same paradigm as above (Figures 2E and 2F). Both sets of experiments (quenching of cypHer-labeled boutons in the presence of Dynasore and destaining of FM-stained boutons in the presence of 30 μM Pitstop 2) yielded near-identical results showing strong STD at 40 Hz. Compared to spH-labeled boutons, the relative responses to the test stimulus are smaller, owing to the fact that αSyt1-cypHer and FM dye inhomogenously label only a fraction of the recycling and resting pools of SVs (Groemer and Klingauf, 2007; Hua et al., 2010). The data show that overexpression of spH does not alter STD and that blocking essential components of compensatory endocytosis causes a prompt and strong STD during high-frequency stimulation. Note that strong STD occurs within 5 s, a time span for which we have shown that SV reuse is negligible.

Recruitment of Reserve SVs during Multiple Spaced Stimuli

When SVs that carry spH are trapped in the alkaline state after a first round of exo-endocytosis, during further stimulation fusion of them will not contribute to the fluorescence increase, which will lead to a progressive reduction in the evoked fluorescence response. Such an effect was consistently observed during multiple rounds of short stimuli in the presence of Folimycin (Li et al., 2005). Similar progressive reduction in response amplitudes was also reported in hippocampal cultures treated with Dynasore (Newton et al., 2006), which was believed to be the consequence of SV pool depletion during sustained activity in the absence of dynamin-dependent endocytosis. To test whether fast SV pool depletion is the cause for fast STD in the presence of Dynasore, we analyzed responses of synapses expressing spH to multiple brief stimuli (50 APs at 20 Hz) at 60 s intervals in the presence of Dynasore, Folimycin, or the delivery vehicle DMSO. Deconvolution was performed on control responses (with DMSO) and showed stepwise increases in cumulative release with identical amplitudes over 10 trials (Figure 3A). When Folimycin was applied, fluorescence responses decreased gradually to about 40% of the initial response (Figure 3B), indicating an increased percentage of alkaline-trapped SVs in the readily releasable pool (RRP). Note that this happens on a timescale much longer than that of the experiment of Figure 1F. In the presence of Dynasore, endocytosed vesicles should be absent and one would expect release sites to be occupied by not yet alkaline-trapped vesicles from the so-called recycling pool (RP). This pool provides a reservoir of several RRPs (Harata et al., 2001; Rizzoli and Betz, 2005). Therefore, response amplitudes similar to those of the DMSO control experiments were expected, except for some decrease later in the recording due to depletion of the RP. Surprisingly, a reduction in response amplitude was observed early-on, which was even stronger than that in the presence of Folimycin. This early decrease cannot be explained by SV depletion, since release sites should be occupied in the absence of endocytosis at least to the same degree as that

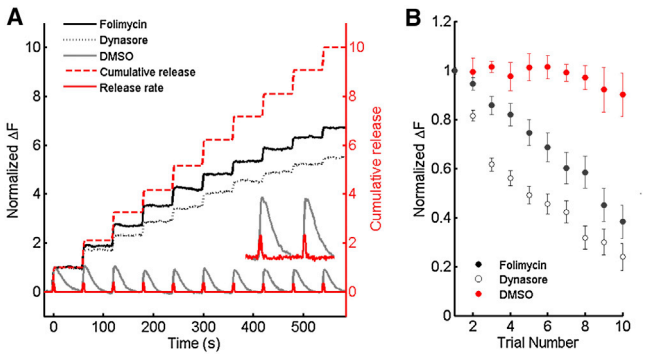

Figure 3. Recruitment of Reserve Vesicles during Multiple Spaced Stimuli

(A) Representative spH responses to consecutive stimuli (50 APs at 20 Hz) with 60 s intervals for recovery (gray) plotted together with the calculated release rate (red solid line) and cumulative release (red broken line). For comparison, the same experiment was repeated in the presence of Folimycin (black solid line) or Dynasore (black broken line). Transients were normalized to first response. Inset: spH transient and calculated release rate during last two stimuli. (B) Plot of changes in signal amplitudes upon each trial. In control, evoked responses (red, n = 3) remain almost constant over at least ten trials, while those of Dynasore (black open cycle) or Folimycin (black closed cycle) treatment decrease to different extents (38.3% ± 7.2% for Folimycin and 23.9% ± 5.5% for Dynasore, n = 6 each). Error bars represent SEM. See also Figure S2.

reported by the acidic SVs in the Folimycin case. Therefore, our data reveal an effect of Dynasore beyond the one caused by insufficient SV supply.

Surface Accumulation of Vesicular Components Caused by Dynasore

Although the major phenotype of genetically impaired dynamin activity is a reduction in the SV pool size and the appearance of coated pits and invaginations at stimulated synapses (Ferguson et al., 2007; Newton et al., 2006), acute block of dynamin activity has been shown to result in STD, which is not readily explained by such long-term effects. Rather, it was postulated that such block of endocytosis may perturb the clearance of vesicle components from release sites, thereby interfering with docking and priming of new SVs (Haucke et al., 2011; Kawasaki et al., 2000; Neher, 2010). Here we took advantage of STED nanoscopy to follow the fate of newly exocytosed SV proteins on the plasma membrane in the presence of Dynasore. Previous STED nanoscopy (Hua et al., 2011) demonstrated that the surface fraction of the SV protein synaptotagmin 1 (Syt1) is enriched at the periphery (potential endocytic site) of synapses at rest. Surface Syt1 is taken up during SV endocytosis and recycled. We, therefore, developed a staining protocol, which simultaneously displays surface-resident and newly exocytosed Syt1 during Dynasore application. We first stained surface Syt1 of live neurons with an antibody against the short Syt1 ectodomain coupled to ATTO 647N at 4°C and in the presence of 1 μM TTX to suppress endocytosis and network activity. We then washed out TTX at room temperature, applied the same antibody coupled to ATTO 590, immediately elicited 200 APs at 20 Hz, and incubated for 15 more min on ice before fixation (Figure 4A). Two

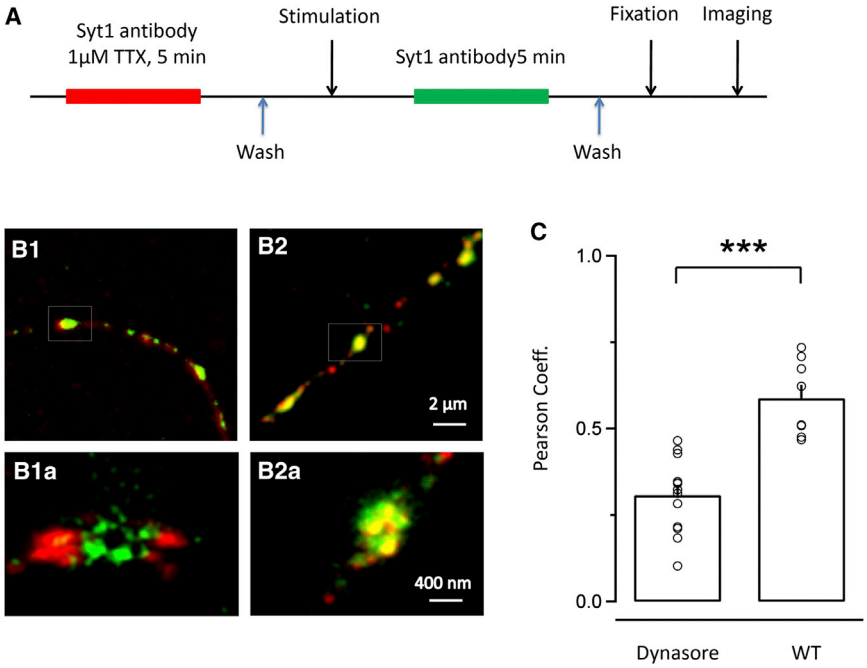

Figure 4. Accumulation of Vesicle Components in the Presence of Dynasore

(A) Experimental protocol for labeling surface-stranded and newly exocytosed Syt1 patches. (B) Representative images of surface-stranded Syt1 (red) and newly exocytosed Syt1 (green) in the presence (B1 and B1a) or absence of Dynasore (B2 and B2a). Overviews (B1 and B2) in confocal mode. Scale bar, 2 µm. STED images at 80 nm lateral resolution (B1a and B2a). Clear spatial separation between Syt1 patches was frequently observed in STED images from experiments performed in the presence of Dynasore (B1a) but not in those from control experiments (B2a), indicating that Dynasore disrupts translocation of newly exocytosed Syt1 toward the RRetP. Scale bar, 400 nm. (C) Pearson coefficients were calculated for images from experiments performed in the presence of either Dynasore or DMSO after background subtraction. A significant reduction was observed in the Dynasore-treated group compared to control (Dynasore = 0.31 ± 0.011, n = 13; WT = 0.59 ± 0.012, n = 8, ***p < 0.001).

populations of Syt1 could be well distinguished using dual-color STED nanoscopy. Without Dynasore (DMSO only) both populations overlapped, indicating proximity between newly exocytosed and pre-existing surface Syt1, which might have been endocytosed during the stimulation period (Figure 4B). Dynasore application, however, led to a clear segregation of both surface pools, with newly exocytosed Syt1 close to release sites (Figures 4B and 4C), suggesting that Dynasore perturbs translocation of vesicular components toward endocytic sites.

DISCUSSION

We investigated the impact of two endocytosis inhibitors, Dynasore and Pitstop, on synaptic release in cultured rat hippocampal neurons using spH, cypHer-labeled antibodies, and styryl dyes as reporters. Our results demonstrate a coupling between endocytosis and exocytosis, such that proper function of endocytic proteins is required for sustained exocytosis during high-frequency stimulation. Upon inhibition of endocytosis, the capacity of the synapse to quickly remove material from the release site, whether actively or passively, seems to be obstructed as the synapse becomes saturated with vesicular debris, disrupting the function of the release machinery and leading to STD.

In order to perform quantitative measurements we designed a normalization and deconvolution strategy of spH responses, providing estimates of the cumulative release without any pharmacological perturbations, such as alkaline-trapping. Deconvolution distinguishes itself from alkaline-trapping by counting contributions of all vesicles, including reused ones, that alkaline-trapping fails to register. Therefore, it is an excellent tool for quantifying SV reuse. In fact, we found no preferential reuse of exocytosed SVs under mild stimulation (up to 200 APs within 40 s; Figures 1F and 2A). The amount of cumulative release upon 200 APs appeared to be insensitive to variations in stimulation frequency up to 40 Hz, which may be a consequence of the activity-dependent replenishment of RRP described earlier (Dittman and Regehr, 1998; Stevens and Wesseling, 1998; Wang and Kaczmarek, 1998). We conclude that fast RRP replenishment from the preexisting RP alone can guarantee a sufficient SV supply during short periods of physiological stimulation, without additional contributions of rapidly reused SVs.

The measured cumulative release under a variety of stimulation conditions (Figure 2) allowed probing STD caused by acute block of dynamin activity. Consistent with previous work at the Calyx of Held (Hosoi et al., 2009), we found that perturbation of dynamin function led to a significant reduction in the cumulative release during high-frequency (40 Hz) stimulation. When the same number of stimuli was applied at a lower rate, STD was almost undetectable. It has been postulated that insufficient SV supply accounts for such STD in Dynasore-treated neurons (Newton et al., 2006), since depletion of fusion competent SVs is a direct consequence of impaired endocytosis under inhibition of dynamin. However, our results challenge this view, since alkaline-trapping experiments show that even during high-frequency stimulation for up to a few tens of seconds (Figure 2A), SVs are mainly recruited from the pre-existing SV pool. It should be noted that in these experiments Dynasore was applied only 5 min before recording, to avoid chronic changes, such as depletion of SVs in the synaptic bouton, as reported in studies, where the protein was genetically ablated (Lou et al., 2012).

Is it specifically dynamin that figures in a yet unknown step immediately postfusion to prevent STD, well before its role in clathrin-coated SV scission? Or does Dynasore nonspecifically induce STD or else does any form of blocking endocytosis

lead to deeper STD? We also targeted another pivotal process in between exo- and endocytosis, namely, clathrin-mediated pit formation, with the membrane-permeable variant of Pitstop (von Kleist et al., 2011) and found that this resulted in the same fast STD, qualitatively and quantitatively. Thus, two completely different maneuvers, interfering with early and late steps of compensatory endocytosis, somehow cause a reduction in release with a time constant in the same subsecond range, much shorter than that of SV fission during endocytosis (5–20 s). This effect manifests itself, once the dynamin or clathrin activity is abolished. What step could this be? As previously proposed (Haucke et al., 2011; Kawasaki et al., 2000; Neher, 2010), translocation of synaptic components from sites of exocytosis to a "periactive zone" (Roos and Kelly, 1999) is a good candidate for this step. This is supported by findings that perturbations of dynamin and several interacting proteins enhance STD upon high-frequency stimulation (Hosoi et al., 2009; Marie et al., 2004). These studies include intersectin, which interacts with the actin regulatory proteins neural wiskott-Aldrich syndrome protein (nwASP) and cell division control protein 42 (CDC42) (Pechstein et al., 2010). Therefore, perturbing endocytosis, through inhibition of either dynamin or clathrin, leads to the accumulation of vesicular components around release sites (Figure 4) due to the lack of free endocytic sites. This prevents previously used release sites from participating in the recruitment of readily releasable SVs. Free diffusion of exocytosed SV proteins on the plasma membrane may account for the slow restoration of release sites after endocytosis block. Accordingly, less STD was observed when release probability and surface protein accumulation, respectively, was artificially reduced by lowering external calcium concentration (Figure S4). Moreover, it has been reported that during high-frequency stimulation of mouse motor nerve terminals, sites of endocytosis were found much closer to the release sites than during mild stimulation (Gaffield et al., 2009). If this is also the case for cultured hippocampal neurons, deeper STD might be expected for high-frequency stimulation due to protein crowding around release sites. At physiological temperature, however, the release site clearance may substantially speed up and thereby STD may not show up until higher stimulation frequencies are applied.

In conclusion, our study demonstrates that impaired endocytosis leads to a novel form of fast STD, which is not related to insufficient vesicle supply at the presynaptic bouton, but is a result of slow clearance of vesicular components from the release site. This finding implies an important role of endocytic proteins for sustained synaptic transmission at high rates beyond their well-established roles in early and late steps of endocytosis.

EXPERIMENTAL PROCEDURES

Cell Culture

Primary cultures (~5000–7500 cells per coverslip) were prepared from the CA3-CA1 region of 1-day-old Wistar rats according to the regulations of the University of Münster/Max-Planck Society and as described (Goslin and Banker, 1991). Transfection of superecliptic spH was performed at 3 days in vitro (DIV) by a modified calcium phosphate transfection procedure. All imaging experiments were carried out at 14–21 DIV at room temperature (20–25°C).

Immunofluorescence and FM Staining

CypHer-conjugated Syt1-antibody (mouse monoclonal, 604.2, Synaptic Systems) was used to label hippocampal neurons. Neurons were incubated with staining buffer (1:200) at 37°C for 3–4 hr in a bicarbonate buffer containing 120 mM NaCl, 5 mM KCl, 2 mM $MgCl_2$, 2 mM $CaCl_2$, 10 mM glucose, and 18 mM $NaHCO_3$, pH 7.4. The culture was then washed with antibody-free buffer twice before use. For FM dye staining, cells were challenged by electric field stimulation (600 APs at 10 Hz) in the presence of 5 μM FM1-43.

Epifluorescence Microscopy

Coverslips were placed in a perfusion chamber containing a modified Tyrode solution (in mM: 120 NaCl, 2.5 KCl, 2 $CaCl_2$, 2 $MgCl_2$, 10 Glucose, 10 HEPES, pH 7.4). For electric field stimulation 1 ms pulses of 50 mA and alternating polarity, applied by a constant current stimulus isolator (WPI A 385, World Precision Instruments), were delivered via two platinum electrodes spaced at 10 mm; 10 μM 6-cyano-7-nitroquinoxaline-2, 3-dione (CNQX) and 50 μM D, l-2-amino-5-phosphonovaleric acid (AP5) were added to prevent recurrent activity. Note that for FM destaining experiments 200 μM Advasep was added to the solution to prevent fast reuptake at high frequencies. Folimycin A (Merck Chemicals Ltd.), Dynasore (Sigma-Aldrich, Germany), and Pitstop 2 (prepared by Volker Haucke) were stored frozen in 20 μl aliquots (1000×) and diluted before use to a final concentration of 80 nM, 100 μM, and 30 μM, respectively, in DMSO.

Fluorophores were excited at 488 nm (spH and FM1-43) or 645 nm (cypHer) with a computer-controlled monochromator (Polychrom IV, Till Photonics). Time-lapse images were acquired using an electron-multiplying CCD camera (iXon+ DU-897E-BV; Andor Technology), which was controlled by iQ software (Andor Technology) and mounted on an inverted Nikon TE2000 microscope equipped with a 60×, 1.2 numerical aperture water-immersion objective and an FITC/Cy5 dual-band filter set (AHF analysentechnik AG). Images were analyzed using a self-written program in Matlab (MathWorks) as previously described (Hua et al., 2011).

Dual-Color STED Nanoscopy

Dual-color STED images were recorded with a custom-built STED-nanoscope that combines two pairs of excitation and STED laser beams, all derived from a single supercontinuum laser source as described (Bückers et al., 2011). STED images were processed using a linear deconvolution that was performed according to the Richardson-Lucy algorithm using a regularization parameter of 10^{-10} and performing 15 iterations. The point spread function for deconvolution was generated by using a 2D Lorentz function with its half-width and half-length fitted to the half-width and half-length of each individual image. Both Syt1 antibodies (mouse monoclonal, 604.2, Synaptic Systems) were directly labeled with either ATTO 647N or ATTO 590 and diluted (1:200) with Tyrode solution before use. For surface pool staining, neurons were preincubated in 1 μM TTX at room temperature for 15 min. Antibody stainings were performed for 15 min on ice to suppress endocytosis. Stimulation in between stainings, however, had to be performed at room temperature. Cells were washed twice and fixed for 15 min in 4% PFA.

SUPPLEMENTAL INFORMATION

Supplemental Information includes four figures and can be found with this article online at http://dx.doi.org/10.1016/j.neuron.2013.08.010.

ACKNOWLEDGMENTS

We thank I. Herfort for the preparation of hippocampal neuron cultures and Drs. Roman Schmidt, Johanna Bückers, and Stefan Hell (MPI for Biophysical Chemistry, Göttingen, Germany) for their great help with dual-color-STED imaging. Y.H. was supported by a stipend from the Max-Planck Society. A.W. was funded through the Cluster of Excellence and DFG Research Center Nanoscale Microscopy and Molecular Physiology of the Brain. V.H. was funded by the DFG (SFB 958/A01). E.N. was supported by a grant from the European Commission (Health-F2-2009-241498; Eurospin). J.K. was

supported by grants from the DFG (ESF Euromembrane, SFB 629, SFB 944, and DFG EXC 1003, Cells in Motion Cluster of Excellence, Münster, Germany).

Accepted: August 13, 2013
Published: October 16, 2013

REFERENCES

Ariel, P., and Ryan, T.A. (2010). Optical mapping of release properties in synapses. Front Neural Circuits *4*, 18.

Balaji, J., and Ryan, T.A. (2007). Single-vesicle imaging reveals that synaptic vesicle exocytosis and endocytosis are coupled by a single stochastic mode. Proc. Natl. Acad. Sci. USA *104*, 20576–20581.

Betz, W.J., and Bewick, G.S. (1993). Optical monitoring of transmitter release and synaptic vesicle recycling at the frog neuromuscular junction. J. Physiol. *460*, 287–309.

Bückers, J., Wildanger, D., Vicidomini, G., Kastrup, L., and Hell, S.W. (2011). Simultaneous multi-lifetime multi-color STED imaging for colocalization analyses. Opt. Express *19*, 3130–3143.

Dittman, J.S., and Regehr, W.G. (1998). Calcium dependence and recovery kinetics of presynaptic depression at the climbing fiber to Purkinje cell synapse. J. Neurosci. *18*, 6147–6162.

Ferguson, S.M., Brasnjo, G., Hayashi, M., Wölfel, M., Collesi, C., Giovedi, S., Raimondi, A., Gong, L.W., Ariel, P., Paradise, S., et al. (2007). A selective activity-dependent requirement for dynamin 1 in synaptic vesicle endocytosis. Science *316*, 570–574.

Fernández-Alfonso, T., and Ryan, T.A. (2004). The kinetics of synaptic vesicle pool depletion at CNS synaptic terminals. Neuron *41*, 943–953.

Gaffield, M.A., Tabares, L., and Betz, W.J. (2009). Preferred sites of exocytosis and endocytosis colocalize during high- but not lower-frequency stimulation in mouse motor nerve terminals. J. Neurosci. *29*, 15308–15316.

Goslin, K., and Banker, G. (1991). Culturing Nerve Cells (Cambridge, MA, USA: MIT Press).

Groemer, T.W., and Klingauf, J. (2007). Synaptic vesicles recycling spontaneously and during activity belong to the same vesicle pool. Nat. Neurosci. *10*, 145–147.

Harata, N., Ryan, T.A., Smith, S.J., Buchanan, J., and Tsien, R.W. (2001). Visualizing recycling synaptic vesicles in hippocampal neurons by FM 1-43 photoconversion. Proc. Natl. Acad. Sci. USA *98*, 12748–12753.

Haucke, V., Neher, E., and Sigrist, S.J. (2011). Protein scaffolds in the coupling of synaptic exocytosis and endocytosis. Nat. Rev. Neurosci. *12*, 127–138.

Hosoi, N., Holt, M., and Sakaba, T. (2009). Calcium dependence of exo- and endocytotic coupling at a glutamatergic synapse. Neuron *63*, 216–229.

Hua, Y., Sinha, R., Martineau, M., Kahms, M., and Klingauf, J. (2010). A common origin of synaptic vesicles undergoing evoked and spontaneous fusion. Nat. Neurosci. *13*, 1451–1453.

Hua, Y., Sinha, R., Thiel, C.S., Schmidt, R., Hüve, J., Martens, H., Hell, S.W., Egner, A., and Klingauf, J. (2011). A readily retrievable pool of synaptic vesicles. Nat. Neurosci. *14*, 833–839.

Kawasaki, F., Hazen, M., and Ordway, R.W. (2000). Fast synaptic fatigue in shibire mutants reveals a rapid requirement for dynamin in synaptic vesicle membrane trafficking. Nat. Neurosci. *3*, 859–860.

Kopp-Scheinpflug, C., Tolnai, S., Malmierca, M.S., and Rübsamen, R. (2008). The medial nucleus of the trapezoid body: comparative physiology. Neuroscience *154*, 160–170.

Kraushaar, U., and Jonas, P. (2000). Efficacy and stability of quantal GABA release at a hippocampal interneuron-principal neuron synapse. J. Neurosci. *20*, 5594–5607.

Li, Z., Burrone, J., Tyler, W.J., Hartman, K.N., Albeanu, D.F., and Murthy, V.N. (2005). Synaptic vesicle recycling studied in transgenic mice expressing synaptopHluorin. Proc. Natl. Acad. Sci. USA *102*, 6131–6136.

Lorteije, J.A., Rusu, S.I., Kushmerick, C., and Borst, J.G. (2009). Reliability and precision of the mouse calyx of Held synapse. J. Neurosci. *29*, 13770–13784.

Lou, X., Fan, F., Messa, M., Raimondi, A., Wu, Y., Looger, L.L., Ferguson, S.M., and De Camilli, P. (2012). Reduced release probability prevents vesicle depletion and transmission failure at dynamin mutant synapses. Proc. Natl. Acad. Sci. USA *109*, E515–E523.

Macia, E., Ehrlich, M., Massol, R., Boucrot, E., Brunner, C., and Kirchhausen, T. (2006). Dynasore, a cell-permeable inhibitor of dynamin. Dev. Cell *10*, 839–850.

Marie, B., Sweeney, S.T., Poskanzer, K.E., Roos, J., Kelly, R.B., and Davis, G.W. (2004). Dap160/intersectin scaffolds the periactive zone to achieve high-fidelity endocytosis and normal synaptic growth. Neuron *43*, 207–219.

Miesenböck, G., De Angelis, D.A., and Rothman, J.E. (1998). Visualizing secretion and synaptic transmission with pH-sensitive green fluorescent proteins. Nature *394*, 192–195.

Neher, E. (2010). What is Rate-Limiting during Sustained Synaptic Activity: Vesicle Supply or the Availability of Release Sites. Front Synaptic Neurosci *2*, 144.

Newton, A.J., Kirchhausen, T., and Murthy, V.N. (2006). Inhibition of dynamin completely blocks compensatory synaptic vesicle endocytosis. Proc. Natl. Acad. Sci. USA *103*, 17955–17960.

Pechstein, A., Shupliakov, O., and Haucke, V. (2010). Intersectin 1: a versatile actor in the synaptic vesicle cycle. Biochem. Soc. Trans. *38*, 181–186.

Rancz, E.A., Ishikawa, T., Duguid, I., Chadderton, P., Mahon, S., and Häusser, M. (2007). High-fidelity transmission of sensory information by single cerebellar mossy fibre boutons. Nature *450*, 1245–1248.

Rizzoli, S.O., and Betz, W.J. (2005). Synaptic vesicle pools. Nat. Rev. Neurosci. *6*, 57–69.

Roos, J., and Kelly, R.B. (1999). The endocytic machinery in nerve terminals surrounds sites of exocytosis. Curr. Biol. *9*, 1411–1414.

Sankaranarayanan, S., De Angelis, D., Rothman, J.E., and Ryan, T.A. (2000). The use of pHluorins for optical measurements of presynaptic activity. Biophys. J. *79*, 2199–2208.

Stevens, C.F., and Wesseling, J.F. (1998). Activity-dependent modulation of the rate at which synaptic vesicles become available to undergo exocytosis. Neuron *21*, 415–424.

Sudhof, T.C. (2004). The synaptic vesicle cycle. Annu. Rev. Neurosci. *27*, 509–547.

von Kleist, L., Stahlschmidt, W., Bulut, H., Gromova, K., Puchkov, D., Robertson, M.J., MacGregor, K.A., Tomilin, N., Pechstein, A., Chau, N., et al. (2011). Role of the clathrin terminal domain in regulating coated pit dynamics revealed by small molecule inhibition. Cell *146*, 471–484.

Wang, L.Y., and Kaczmarek, L.K. (1998). High-frequency firing helps replenish the readily releasable pool of synaptic vesicles. Nature *394*, 384–388.

Wienisch, M., and Klingauf, J. (2006). Vesicular proteins exocytosed and subsequently retrieved by compensatory endocytosis are nonidentical. Nat. Neurosci. *9*, 1019–1027.

Wu, X.S., and Wu, L.G. (2009). Rapid endocytosis does not recycle vesicles within the readily releasable pool. J. Neurosci. *29*, 11038–11042.

Zhou, Q., Petersen, C.C., and Nicoll, R.A. (2000). Effects of reduced vesicular filling on synaptic transmission in rat hippocampal neurones. J. Physiol. *525*, 195–206.